Density Functional Theory Study of the Carbonyl-ene Reaction of Encapsulated Formaldehyde in Cu(I), Ag(I), and Au(I) Exchanged FAU Zeolites

3 **AUTHORS**, INCLUDING:

Sippakorn Wannakao
Kasetsart University
9 PUBLICATIONS **97** CITATIONS

SEE PROFILE

Pipat Khongpracha
Kasetsart University
41 PUBLICATIONS **435** CITATIONS

SEE PROFILE

Density Functional Theory Study of the Carbonyl-ene Reaction of Encapsulated Formaldehyde in Cu(I), Ag(I), and Au(I) Exchanged FAU Zeolites

Sippakorn Wannakao,[†,‡,§] Pipat Khongpracha,[†,‡,§] and Jumras Limtrakul*,[†,‡,§]

[†]Laboratory for Computational and Applied Chemistry, Department of Chemistry, Faculty of Science and Center of Nanotechnology, Kasetsart University Research and Development Institute, Kasetsart University, Bangkok 10900, Thailand

[‡]Center for Advanced Studies in Nanotechnology and Its Applications in Chemical, Food and Agricultural Industries, Kasetsart University, Bangkok 10900, Thailand

[§]NANOTEC Center of Excellence, National Nanotechnology Center, Kasetsart University, Bangkok 10900, Thailand

ⓢ *Supporting Information*

ABSTRACT: Carbonyl-ene reactions, which involve C—C bond formation, are essential in many chemical syntheses. The formaldehyde—propene reaction catalyzed by several of the group 11 metal cations, Cu^+, Ag^+, and Au^+ exchanged on the faujasite zeolite (metal-FAU) has been investigated by density functional theory at the M06-L/6-31G(d,p) level. The Au-FAU exhibits a higher activity than the others due to the high charge transfer between the Au and the reactant molecules, even though it is located at a negatively charged site of the zeolite. This site enables it to compensate for the charge of the Au^+ ion. The NBO analysis reveals that the 6s orbital of the Au atom plays an important role, inducing a charge on the probe molecules. Moreover, the effect of the zeolite framework makes the Au-FAU more active than the others by stabilizing the high charge induced transition structure. The activation energy of the reaction catalyzed by Au-FAU is 13.0 kcal/mol whereas that of Cu and Ag-FAU is found to be around 17 kcal/mol. The product desorption needs to be improved for Au-FAU; however, we suggest that catalysts with high charge transfer might provide a promising activity.
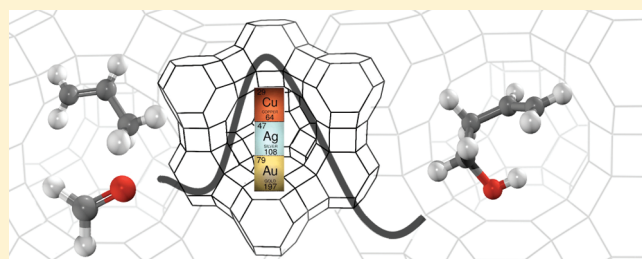
1. INTRODUCTION

Reactions involving carbon—carbon bond formation are essential for most chemical upgrading processes. Among the well-known C—C bond formations, the carbonyl-ene reaction is one of the top choices for synthesis.[1,2] The carbonyl-ene reaction is induced by Lewis acid[3] and generally requires a strongly electrophilic carbonyl compound. The reaction of formaldehyde and propene is an example of the carbonyl-ene reaction that yields as a product 3-buten-1-ol. This product can be used in chemical processes, e.g., the copolymerization of propylene for producing polypropylene. In addition, the formaldehyde—propene reaction is involved in the synthesis of tetrahydrofuran, one of the most popular organic solvents in the laboratory.

Because of its low boiling point (−19.5 °C), formaldehyde is difficult to handle. Moreover, it rapidly polymerizes to solid paraformaldehyde and trioxane. Then, its shelf life is quite short. To retain formaldehyde in its monomer state, Lewis acid treatment is used to depolymerize the polymer form. Unfortunately, the treatment causes problems of corrosion, handling, and toxic waste, making it environmentally unfriendly. For these reasons, formaldehyde has become limited in its application for organic synthesis. Finding storage materials that retain the monomeric formaldehyde should be a way for solving these problems.

Porous materials such as zeolites and metal organic frameworks (MOF),[4−11] a new type of designable material, widely used as gas storage and separation materials, are environmentally friendly candidates for formaldehyde storage. Successful utilization of a porous material for formaldehyde storage was achieved by Okachi et al.[12] in 2004. These authors found that Na/faujasite zeolite suppresses the decomposition and self-polymerization of formaldehyde while its reactivity toward nucleophiles remains the same. Recently, Tomita et al.[13] have theoretically demonstrated that formaldehyde does not tend to self-polymerize in alkaline-exchanged faujasite zeolite. Our previous ONIOM calculation of the formaldehyde-propene reaction on Na-exchanged faujasite zeolite has revealed that alkaline-exchanged zeolite can significantly reduce the reaction barrier in the reaction mechanism

compared to an uncatalyzed process.[14] Thus, it can be suggested not only that zeolite can be used for storage but that alkaline-exchanged zeolite can also enable catalyzation of this reaction. Zeolite can be used for not only these purposes but also metal organic frameworks.

In our recent study, the formaldehyde—propene reaction in MOF-11, in which the active site is Cu(II) in the paddle wheel unit $(Cu_2(CO_2)_4)$, was theoretically investigated.[15] It was found that MOF-11 can reduce the activation energy of the reaction from 34.3 to 24.1 kcal/mol. A bare Cu^+, however, is much more reactive with an activation barrier of only 6.4 kcal/mol. There-fore, MOF-11 can be utilized in catalytic applications only with a moderated activity. Finding a structure that retains the high activity of the metal would be promising, not only for its academic interest but also for industrial applications.

Metals loaded on zeolites have been widely studied as their properties can be fine-tuned by varying the metals. Bell and co-workers have synthesized and characterized Cu(I)-exchange zeolite Y for catalyzing the dimethyl carbonate (DMC) reaction from oxidative carbonylation of methanol.[16−19] They found that Cu—Y provided a high reactivity for the reaction. Moreover, Ag(I) and Au nanoparticles exhibit good performances in reac-tions involving C—C bond formation.[20−22] The monomeric Au cation on zeolites has been successfully prepared,[23−29] and many theoretical studies have been conducted.[30−35] Ichikawa et al.[23,25] used CO adsorption and Fourier transform IR (FTIR) to study Au/NaY, Au/Na-mordenite, and Au/Na-ZSM-5 and concluded that Au(I) is the dominant active site for the decomposition of NO with CO and the water gas shift. Fierro-Gonzalez and Gates[26] have also synthesized and characterized monomeric Au(I) and Au(III) in zeolite NaY without zero valence Au clusters.

There is often little correlation between the catalytic activities of different cations on many reactions, even if the ions are chemically related. Thus, each cation has to be tested either theoretically or experimentally for any reaction of interest. Theoretical studies not only save a great deal of time and money compared to complicated experimental screening, but they also provide insight into why a particular cation has a higher activity, and thus a guide to synthesize the catalyst with the required characteristics. As a consequence, in this work, we investigate the formaldehyde-propene carbonyl-ene reaction on the Cu, Ag, and Au cation exchanged on FAU zeolite (M-FAU, M = Cu, Ag, and Au) by means of density functional theory with the M06-L functional.[36−38] Even though metal cations exchanged in zeolites have been widely studied, to the best of our knowledge, there is no theoretical study for the C—C bond formation processes with this series of metal-exchanged zeolites as a catalyst. This work thus investigates the possibility of using group 11 metal-ex-changed zeolites as highly active catalysts for the carbonyl-ene reaction. We also make a comparison with other Lewis acid catatlysts (MOF-11 and Na-FAU).

2. MODELS AND METHOD

The faujasite zeolite is composed of sodalite building blocks that contain 192T (T is either a Si or an Al atom) atoms in the supercage unit cell.[39] The Cu(I) cation can be located in many different cation-exchange sites, as shown in Figure 1. Site I is located in the hexagonal prism, which is not accessible for the reaction to proceed. Site II is inside the FAU supercage on the hexagonal face and site III is also located in the supercage, but on the four-membered ring of the sodalite cage. An experimental
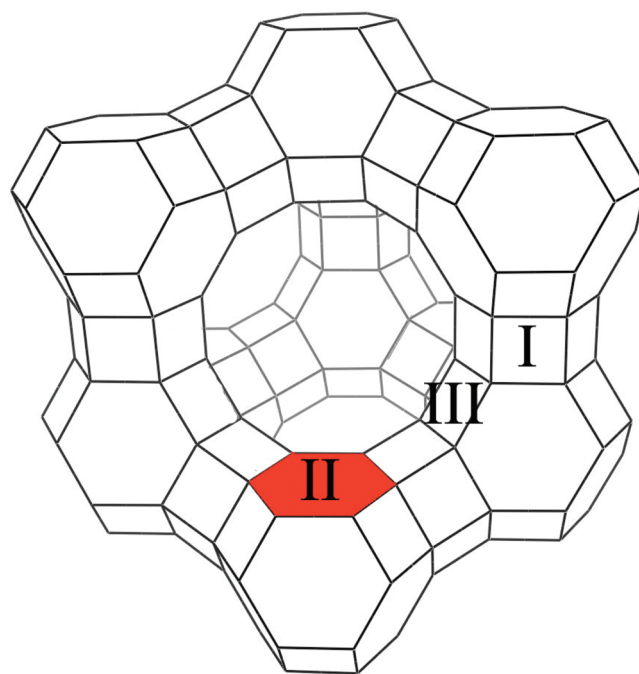
Figure 1. Cation exchanging sites of the faujasite zeolite (see text for explanations).

study by Drake et al.[40] shows that Cu(I) can replace all acidic protons of the H—Y zeolite, resulting in a ratio Cu/Al = 1.0. Moreover, these authors also concluded that site II is the site most occupied by Cu^+ ion. Site II was therefore chosen to represent the catalytically active site in this study. Furthermore, this site has also been studied for other metal cations in several previous reports.[19,30]

The selected 16T model (Figure 2) of site II consists of 6T from the hexagonal ring and the side extended four-membered rings to avoid interaction between terminating hydrogen atoms. To avoid the Al—OH group, which was not observed in experi-ments, Si atoms adjacent to the Al atom were included in the model. The metal ions were located in the middle of the hexagonal ring, as shown in Figure 2. Geometry optimizations were performed at the M06-L/6-31G(d,p) level of theory and Stuttgart ECP[41] were employed for the Cu, Ag, and Au atoms. The M06-L functional has been tested and found to be accurate and affordable from the Minnesota functional series for the energetic properties of systems containing transition metals and even in more sophisticated cases such as metal oxide systems.[37,42−47] Recent studies of chemical reactions regarding zeolite systems has demonstrated that this well calibrated series of functionals provides results in good agreement with experi-mental values.[48−51] Moreover, a theoretical study of the chemical reaction on transition metal oxide-exchanged zeolite shows that the M06-L functional provides acceptable results for both structure and adsorption energies when compared to the MP2[52] method. To avoid too many degrees of freedom during the optimization, only the metal atoms and the 4T region with the three oxygen atoms adjacent to the metal atoms $(-Si_3O_3Al-)$ were allowed to relax while the rest were kept fixed at their crystallographic positions. Transition states were located by the Berny algorithm[53,54] and confirmed by normal-mode analyses that provide only one imaginary frequency corresponding to the designated reaction coordination. Total spin was kept to be singlet
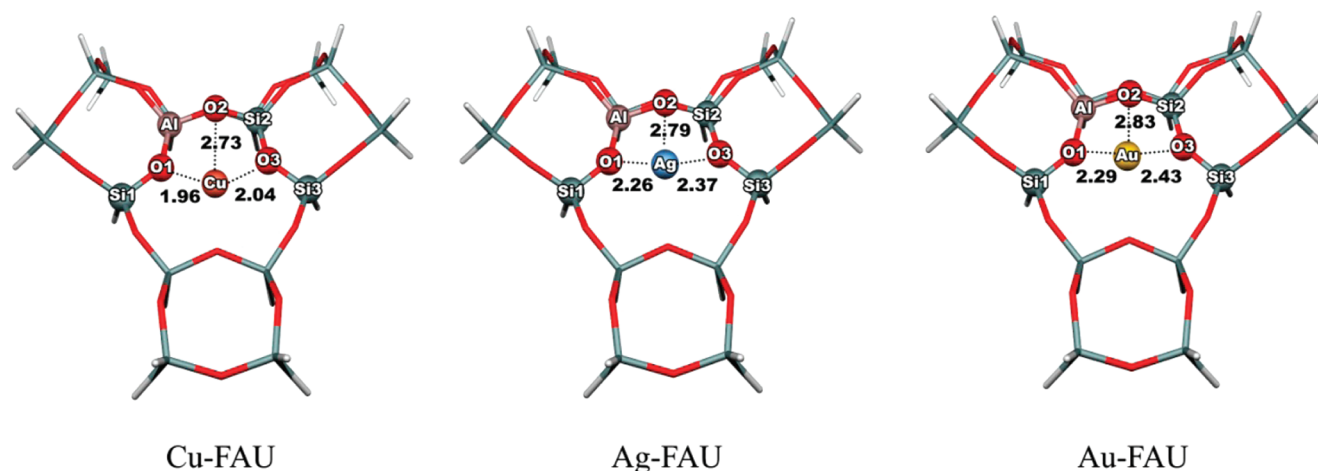
Figure 2. Structures of the Cu-, Ag-, and Au-FAU catalysts obtained from M06-L/6-31G(d,p) optimizations.

Table 1. Partial Electronic Charges of the Metal Atom and the Probe Molecules

		NPA-charges/e		
step		Cu-FAU	Ag-FAU	Au-FAU
catalysts	metal	0.682	0.759	0.699
Ads	C	0.308	0.259	0.327
	O	−0.584	−0.547	−0.557
	HCHO	0.052	0.044	0.141
	metal	0.656	0.707	0.521
CoAds	C	0.217	0.266	0.284
	O	−0.617	−0.589	−0.593
	CoAds	−0.004	0.066	0.161
	metal	0.741	0.666	0.506
TS	C	−0.047	−0.040	−0.070
	O	−0.831	−0.786	−0.759
	TS	0.073	0.077	0.268
	metal	0.632	0.679	0.411

during the reaction pathway for all systems. Interaction between probe molecules and catalysts are reported as relative energies that relative to energies of isolated reactants which can be calculated by the equation, $E = E_{complex} - (E_{reactant1} + E_{reactant2} + ...)$. The charge distributions and population analyses of the complexes were also determined at the M06-L/6-31G(d,p) level of theory by the natural atomic orbital (NAO) and natural bond orbital analysis (NBO) methods.[55,56] The framework was then extended to 120T, covering a supercage structure of FAU, to perform the single point calculation with the same level of theory as the one used for evaluating the effect of the zeolite framework. Zero-point energies were also corrected for the quantum cluster of the 16T model of the zeolite system (Table S3, Supporting Information). All quantum chemical calculations were carried out with the Gaussian 03[57] code, modified to incorporate the Minnesota Density Functionals module 3.1 by Zhao and Truhlar.

3. RESULTS AND DISCUSSION

3.1. Metal-Exchanged Faujasite Zeolite. The optimized structures of the Cu-FAU, Ag-FAU, and Au-FAU models used in this study are illustrated in Figure 2. Partial charges and the electronic configuration of the systems are documented in Table 1 and Table S2 (Supporting Information), respectively. The calculated charges were found to be +0.682e, +0.759e, and +0.699e for the Cu, Ag, and Au atoms, respectively. This shows the compensation between the metal charges and the surrounding oxygen atoms in the 6-membered ring. The complexation energies between the metal cations and the zeolite were found to be −179.2, −147.9, and −154.2 kcal/mol for Cu-, Ag-, and Au-FAU, respectively. It is worth noting that the complexation energies with the amount of charge transfer between M⁺ and the zeolite framework was revealed by the charge reduction of the exchanged cations ($Cu^+ > Au^+ > Ag^+$).

The structures and mechanisms of the encapsulated formaldehyde metal-FAU carbonyl-ene reaction are now investigated. The symbol M@S signifies that the molecule M is adsorbed on the active site S. The proposed reaction mechanism is similar to those of our previous calculations for Na-FAU catalyst as well as for MOF-11. The reaction is assumed to proceed on a concerted mechanism in which both reactants are involved in the rate limiting step. All optimized geometries are given in the Supporting Information, Table S1.

3.2. Encapsulated Formaldehyde in Metal-FAU. To keep formaldehyde in its monomer state and to keep it activated, the reaction begins with the encapsulation of formaldehyde on the metal-FAU catalysts like in the previous studies.[14,15] The oxygen atom of formaldehyde interacts with the Lewis acid metal site of the catalyst. The C—O distance is elongated from 1.20 to 1.23 Å, which is the same as in the alkaline exchange and the MOF-11 studies. The adsorption energies are found to be −16.9, −18.0, and −20.0 kcal/mol for Cu-, Ag-, and Au-FAU, respectively. From the NBO calculations we find highly ionic bonding characteristics between the Au and the O atom of the formaldehyde molecule, formed by the 6s orbital (8.45%) of the Au atom and the 2p orbital (91.55%) of the O atom (Figure 3). The interaction between the O and the Cu or Ag contains a contribution from the lone pair electron of the O atom to the metal (Figure 4). An electron back-donation from the metal to formaldehyde could not be observed at any significant level. The total occupancy of the Cu and Ag atoms were nearly unchanged whereas the Au atom received more electrons at the 6s orbital after the formaldehyde was encapsulated. This might be due to
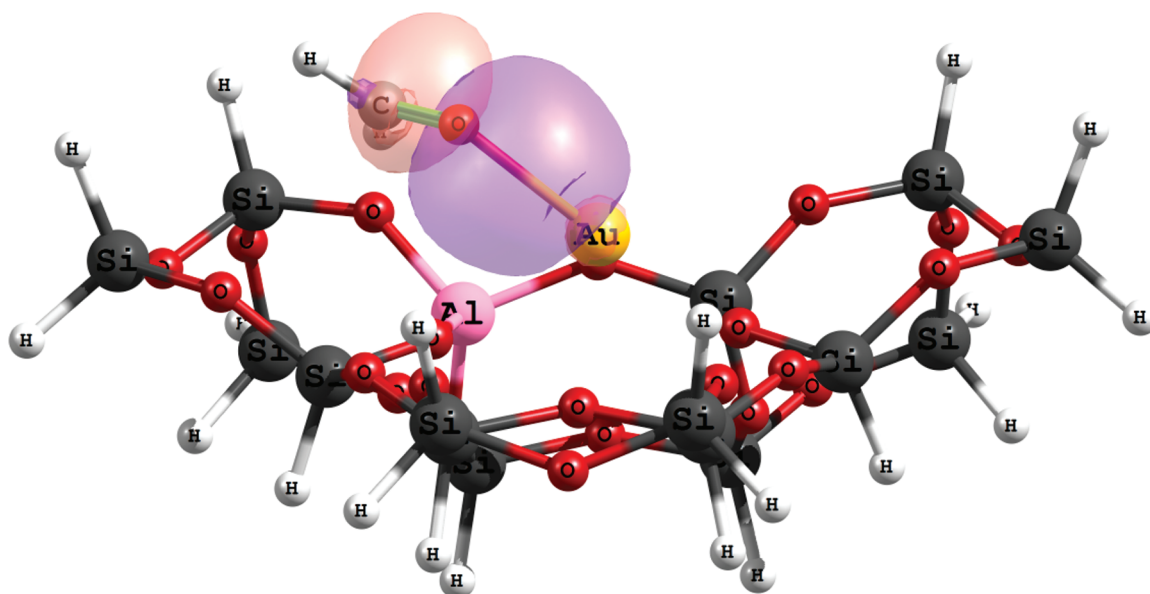
Figure 3. Illustration of the Au—O bonding character with contributions from (mostly) the 6s orbital of Au and the 2p orbital of the O atom. From the NBO calculations with the M06-L/6-31G(d,p) method.


HCHO@Cu

HCHO@Ag
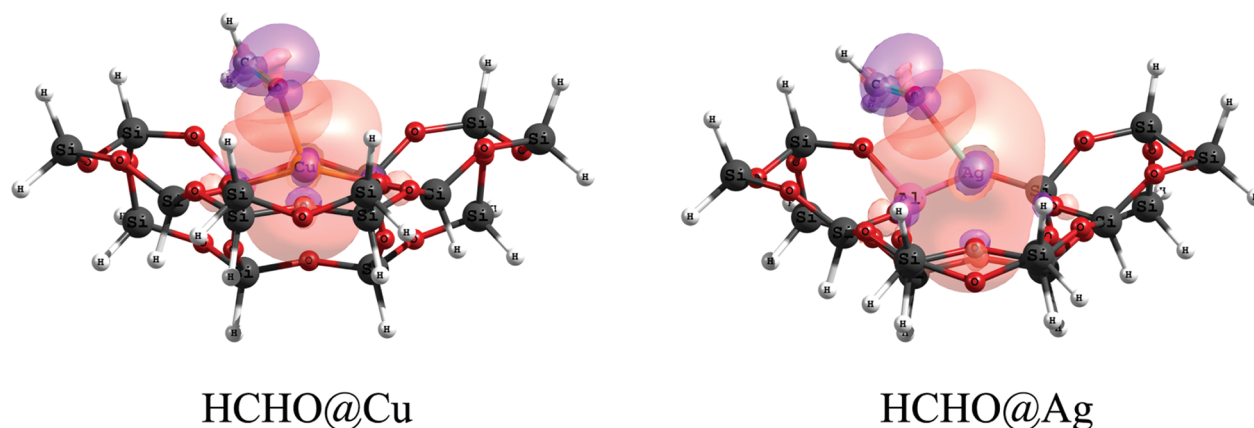
Figure 4. Illustration of the interaction between the 2p orbital of formaldehyde and the 4s orbital of Cu (left)/the 5s orbital of the Ag (right), analyzed from the NBO calculation with the M06-L/6-31G(d,p) method. The isosurface value is ±0.03 au.

the relativistic effect of a heavy metal atom like Au. Moreover, this may be the origin of the shorter length of the Au—O bond (2.26 Å) compared with the Ag—O bond (2.36 Å). The short Cu—O bond (2.07 Å) might originate from the smallest cation size of Cu when compared to that of others. The charge of the formaldehyde carbon atom was found to be +0.308e, +0.259e, and +0.327e in the Cu-, Ag-, and Au-FAU system, respectively. This indicates that Au-FAU causes the formaldehyde molecule to become an active electrophile, as a result the carbon of the HCHO@Au-FAU system favors the nucleophilic attack of another molecule.

An attempt has been made for predicting the carbonyl (CO) stretch vibrational frequencies of formaldehyde and its complexes with different Cu-, Ag-, and Au-FAU zeolites. Without scaling factors, our calculated CO vibrational frequencies of metal(I)/FAU complexes are predicted to be 1723, 1784, and 1747 cm^{-1} for Cu-FAU, Ag-FAU, and Au-FAU, respectively. For all the studied complexes, the carbonyl (CO) stretch vibration is

red-shifted by 85—146 cm^{-1} with respect to the CO vibrational frequency (1869 cm^{-1}) in formaldehyde (cf. Table S4, Supporting Information). These values are higher than those calculated and experimental values for Cu and Ag embedded in other related types of zeolite, i.e., Cu and Ag-ZSM-5 reported by Datka et al.[58,59] However, our calculated C—O distances are longer for Cu- and Ag-FAU cases. This reflects one of the reasons the frequencies of our FAU zeolite are over shifted when compared to those values obtained from ZSM-5.

Metal cations without the zeolite structure (bare-metal cations) were investigated for comparison. The metal cations bind to the formaldehyde molecule with adsorption energies of −48.8, −32.2, and −38.8 kcal/mol for Cu$^+$, Ag$^+$, and Au$^+$, respectively. These energies correspond to the distance between the metal and the oxygen atom of the formaldehyde molecule, where Cu—O < Au—O < Ag—O (1.88, 2.20, and 2.23 Å). When the cations are adsorbed on the zeolite framework, the adsorption energies do not follow this trend due to the compensation

12489

dx.doi.org/10.1021/jp205985v |*J. Phys. Chem. A* 2011, 115, 12486–12492
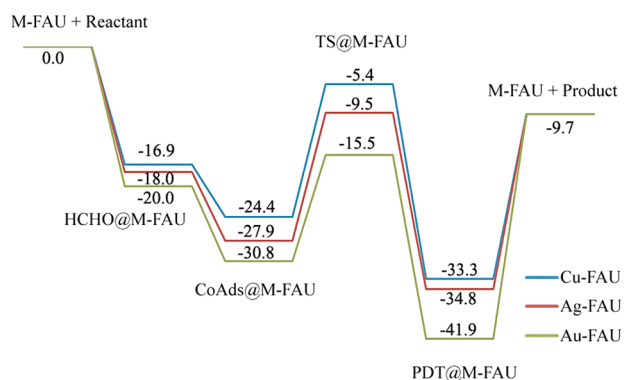
Figure 5. Zero-point corrected energy profiles of the reaction calculated by the 16T M06-L/6-31G(d,p) level of theory (all energies in kcal/mol).

charge transfer between the metals and the zeolite that we mentioned above. However, a large charge transfer character between formaldehyde and metal exchanged zeolite is still exhibited for the Au-FAU; it provides the highest adsorption energy. This indicated a good encapsulation capability of the formaldehyde even in a charge transferable solid support.

3.3. Carbonyl-ene Reaction between Encapsulated Formaldehyde in Metal-FAU and Propene. After the formaldehyde encapsulation, the reaction is followed by the coadsorption of propene to the encapsulated complex and then by a concerted transition state. The energetic reaction profile is summarized in Figure 5. In the coadsorption step, the propene bound to the encapsulated formaldehyde with the coadsorption energy increases by ~10 kcal/mol compared to the formaldehyde adsorption energies in all cases. The charge of the formaldehyde carbon atom is +0.217e, +0.266e, and +0.284e for the Cu-, Ag-, and Au-FAU, respectively. This again indicates that the formaldehyde carbon atom of the Au-FAU is ready to be attacked by the nucleophilic group. Propene and the encapsulated formaldehyde form a concerted transition structure in which new C—C1 and O—H bonds are formed simultaneously and the C3—H bond breaks (Table S1).

The C—O bond of formaldehyde is elongated from 1.23 Å to about 1.35 Å for the Cu and Ag systems whereas the one of the Au system is longer, 1.38 Å. This is compatible with the lowest activation energy for the reaction in Au-FAU, 15.3 kcal/mol, compared to 19.0 and 18.5 kcal/mol of that in Cu- and Ag-FAU, respectively. These results correlate well with the study of the same reaction with several Lewis acid catalysts by Yang et al.[60] They found that an electron withdrawing group at the formaldehyde C atom (providing a higher positive charge of the C atom) leads to a lower activation barrier for the reaction. In our case, the formaldehyde C atom is strongly induced to be highly positive by the metal cations. Moreover, these authors also showed that a more positive charge of the secondary C atom of propene, at the transition state, corresponds to a lower activation barrier. From our calculations, the charges of the propene secondary C atom at the transition state were +0.077e, +0.052e, and +0.157e for the Cu-, Ag-, and Au-FAU systems, respectively. The NBO analysis illustrates that the occupancy of the Au atom is almost unchanged when the propene is coadsorbed. Interestingly, the 6s orbital of the Au atom gains a significant occupation, from 0.45e to 0.59e, whereas the occupancies of Cu and Ag atoms remain almost unchanged when the reaction crosses the transition state.

Table 2. Relative Energies with Respect to the Reactants of the Systems and Desorption Energies (E_{des}) and Activation Energies (E_a) Calculated with 16T/M06-L/6-31G(d,p), 120T/M06-L/6-31G(d,p)//16T/M06-L/6-31G(d,p), and Bare-Metal Systems//16T/M06-L/6-31G(d,p) without Zero-Point Energy Corrections

|	relative energies (kcal/mol)								
	Cu-FAU			Ag-FAU			Au-FAU		
	16T	120T	bare	16T	120T	bare	16T	120T	bare
Ads	−16.5	−20.0	−45.0	−19.0	−21.1	−30.0	−21.6	−24.5	−37.7
CoAds	−27.3	−32.7	−58.2	−30.6	−34.2	−41.7	−33.9	−38.1	−52.6
TS	−8.4	−15.4	−49.3	−12.5	−17.0	−29.5	−18.9	−25.1	−46.6
PDT	−39.7	−48.3	−72.1	−41.0	−46.2	−56.0	−48.8	−55.1	−65.2
E_{des}	24.7	33.3	57.1	26.0	31.2	41.0	33.8	40.1	50.2
E_a	18.9	17.4	8.8	18.0	17.2	12.2	15.0	13.0	6.1
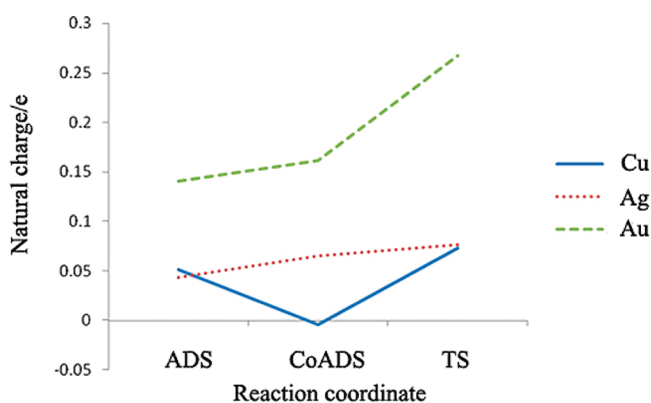
Figure 6. Evolution of the charge of the probe molecules (formaldehyde and propene) along the reaction coordinate.

Consequently, the relativistic effect, which can be inferred from the 6s orbital of the Au atom, might play an important role in the high activity of the Au system. The Au-FAU might have a problem with a high desorption energy (Table 2) when the full catalytic cycle is considered. However, we suggest that the catalyst that is active for this kind of reaction should have a character of high charge transfer to stabilize and activate the formaldehyde monomer.

We furthermore analyze the charges of the probe molecules bound to the metal-FAU systems (Table 1). The results show that the Au atom induces the highest charge of the probe molecules, in all cases and especially for the transition state, where the charge is +0.268e. With the Cu and Ag cations, the metals cannot induce charges of more than +0.100e in an elementary step. The charge evolution during the reaction pathway is shown in Figures 6 and 7.

3.4. Zeolite Framework Effect. In studies of zeolite systems, the framework effect, which contributes the confining van der Waals interactions, is found to be one of the important keys for understanding the adsorption phenomena and the catalytic activity. The extended 120T of the supercage structure of the faujasite zeolite was used for single point calculations to study the effects of the framework. The relative energies of the systems involved in the reaction are summarized in Table 2. We find that all systems are stabilized by the zeolite framework. Interestingly,
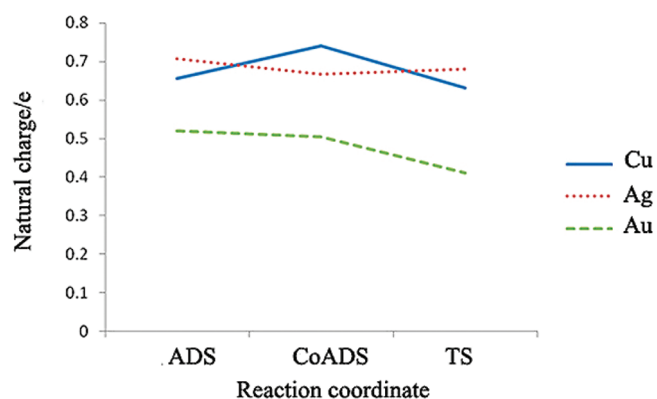
Figure 7. Evolution of the charge of the metal atoms along the reaction coordinate.

the Au-FAU framework structure reduces the activation barrier to only 13.0 kcal/mol and those of the Cu- and Ag-FAU systems remain around 17 kcal/mol (Table 2). This is consistent with a large induced charge flow from the Au atom and with the observation that the zeolite framework is more effective when the reaction proceeds via the ion pair intermediate.[48,61−65] From these results, one can state that the Au cation should work well for reactions promoted by Lewis acids in zeolite frameworks.

We also investigated systems without a zeolite framework. To avoid the effect of structural differences, single point calculations were performed on the optimized structures, but only with the metals and probe fragments (Table 2). The adsorption energies of the formaldehyde on the bare cations (−45.0, −30.0, and −37.7 kcal/mol for Cu, Ag, and Au) were found to be close to the optimized ones (−48.8, −32.2, and −38.8 kcal/mol). In comparison with our previous calculation on the bare-Cu^+ with the B3LYP functional,[15] we found that the single point calculations for the energetic profile of the Cu^+ ion were almost the same as the optimized one with B3LYP, especially the relative energy of the transition state ($\sim$−49 vs −50 kcal/mol). This indicates that the structural difference does not affect the energetic properties as much as the effect of the charge compensation mentioned above. The activation energies of the extreme cases of metal cation systems were calculated to be 8.8, 12.2, and 6.1 kcal/mol for the Cu^+, Ag^+, and Au^+, respectively. Therefore, it can be concluded that the Au^+ ion shows a high activity for this reaction even after charge distribution between the cation and the zeolite occurred.

3.5. Comparison with the Na-FAU and MOF-11 Systems. From our previous study of the Na-exchanged FAU zeolite, we found that this alkaline exchanged zeolite can reduce the activation barrier from $\sim$34 kcal/mol for the uncatalyzed process to $\sim$25 kcal/mol. In comparison, the adsorption and coadsorption energies of the Na-FAU system were close to the results obtained for the transition metal exchanged systems. However, the transition metals provided higher activities by lowering the energy of the transition state, especially for the Au-FAU system. In contrast to the transition metals, the charge of Na was almost unchanged ($\sim$+0.9e) during the whole reaction pathway whereas the charge transfers between the metals and probes are known to play an important role in the activity of transition metal exchanged zeolites.

The Cu site of the MOF-11 has also been used to catalyze this reaction. However, the activation energy was $\sim$24 kcal/mol

whereas that of the bare Cu^+ ion was only 6.4 kcal/mol. This indicates that the MOF-11 structure cannot retain the high activity of the Cu^+ ion. In this work, the zeolite structure was found to be the more appropriate structure for loaded metal to catalyze this kind of reaction.

4. CONCLUSION

The carbonyl-ene reaction over Cu-, Ag-, and Au-exchanged FAU zeolites was investigated in quantum mechanical calculations with an efficient functional, M06-L. The Au^+ ion exhibits a high performance in the formaldehyde encapsulation process and shows a high catalytic activity. By analyzing the electronic configuration, we demonstrated that the 6s orbital of the Au atom plays an important role in this interestingly high activity: It accepts an electron and induces a large charge in the probe molecules. This inductive effect is enhanced by the framework of zeolite. Although the activity of the Cu- and Ag-FAU was not as high as that of the Au-FAU, the zeolite structures are suitable for use as a catalyst for this type of reaction. Moreover, these transition metals provide a higher activity than that of the alkaline-exchanged zeolites, which showed no significant charge transfer. In summary: the cation, which can maintain a charge transfer even in the presence of a charge compensating support is the most appropriate one for this reaction. From our results, we suggest that the Au-exchanged zeolites could be a potential catalyst for this type of reactions. However, the problem of high desorption energy should be improved for industrial applications.

■ ASSOCIATED CONTENT

S **Supporting Information.** Optimized geometries, electronic structures, zero-point energies, and vibrational frequencies. This information is available free of charge via the Internet at http://pubs.acs.org.

■ AUTHOR INFORMATION

Corresponding Author
*E-mail: jumras.l@ku.ac.th. Tel: +66-2-562-5555, ext 2159.

■ ACKNOWLEDGMENT

■ REFERENCES

(1) Hoffmann, H. M. R. *Angew. Chem., Int. Ed. Engl.* **1969**, *8*, 556–577.

(2) Oppolzer, W.; Snieckus, V. *Angew. Chem., Int. Ed.* **1978**, *17*, 476–486.

(3) Yamanaka, M.; Mikami, K. *Helv. Chim. Acta* **2002**, *85*, 4264–4271.

(4) Düren, T.; Sarkisov, L.; Yaghi, O. M.; Snurr, R. Q. *Langmuir* **2004**, *20*, 2683–2689.

(5) Eddaoudi, M.; Kim, J.; Rosi, N.; Vodak, D.; Wachter, J.; O'Keeffe, M.; Yaghi, O. M. *Science* **2002**, *295*, 469–472.

(6) Frost, H.; Snurr, R. Q. *J. Phys. Chem. C* **2007**, *111*, 18794–18803.

(7) Furukawa, H.; Ko, N.; Go, Y. B.; Aratani, N.; Choi, S. B.; Choi, E.; Yazaydin, A. O.; Snurr, R. Q.; O'Keeffe, M.; Kim, J.; et al. *Science* **2010**, *329*, 424–428.

(8) Li, H.; Eddaoudi, M.; O'Keeffe, M.; Yaghi, O. M. *Nature* **1999**, *402*, 276–279.

(9) Rosi, N. L.; Eckert, J.; Eddaoudi, M.; Vodak, D. T.; Kim, J.; O'Keeffe, M.; Yaghi, O. M. *Science* **2003**, *300*, 1127–1129.

(10) Rowsell, J. L. C.; Yaghi, O. M. *Microporous Mesoporous Mater.* **2004**, *73*, 3–14.

(11) Yaghi, O. M.; O'Keeffe, M.; Ockwig, N. W.; Chae, H. K.; Eddaoudi, M.; Kim, J. *Nature* **2003**, *423*, 705–714.

(12) Okachi, T.; Onaka, M. *J. Am. Chem. Soc.* **2004**, *126*, 2306–2307.

(13) Tomita, M.; Masui, Y.; Onaka, M. *J. Phys. Chem. Lett.* **2010**, *1*, 652–656.

(14) Sangthong, W.; Probst, M.; Limtrakul, J. *J. Mol. Struct.* **2005**, *748*, 119–127.

(15) Choomwattana, S.; Maihom, T.; Khongpracha, P.; Probst, M.; Limtrakul, J. *J. Phys. Chem. C* **2008**, *112*, 10855–10861.

(16) Zhang, Y.; Bell, A. T. *J. Catal.* **2008**, *255*, 153–161.

(17) Zhang, Y.; Briggs, D. N.; de Smit, E.; Bell, A. T. *J. Catal.* **2007**, *251*, 443–452.

(18) Zhang, Y.; Drake, I. J.; Briggs, D. N.; Bell, A. T. *J. Catal.* **2006**, *244*, 219–229.

(19) Zheng, X.; Bell, A. T. *J. Phys. Chem. C* **2008**, *112*, 5043–5047.

(20) Baba, T.; Iwase, Y.; Inazu, K.; Masih, D.; Matsumoto, A. *Microporous Mesoporous Mater.* **2007**, *101*, 142–147.

(21) Sakurai, H.; Tsunoyama, H.; Tsukuda, T. *J. Organomet. Chem.* **2007**, *692*, 368–374.

(22) Tsunoyama, H.; Sakurai, H.; Ichikuni, N.; Negishi, Y.; Tsukuda, T. *Langmuir* **2004**, *20*, 11293–11296.

(23) Mohamed, M. M.; Salama, T. M.; Ichikawa, M. *J. Colloid Interface Sci.* **2000**, *224*, 366–371.

(24) Mohamed, M. M.; Salama, T. M.; Ohnishi, R.; Ichikawa, M. *Langmuir* **2001**, *17*, 5678–5684.

(25) Qiu, S.; Ohnishi, R.; Ichikawa, M. *J. Phys. Chem.* **1994**, *98*, 2719–2721.

(26) Fierro-Gonzalez, J. C.; Gates, B. C. *J. Phys. Chem. B* **2004**, *108*, 16999–17002.

(27) Gao, Z. X.; Sun, Q.; Chen, H. Y.; Wang, X.; Sachtler, W. M. H. *Catal. Lett.* **2001**, *72*, 1–5.

(28) Salama, T. M.; Shido, T.; Ohnishi, R.; Ichikawa, M. *J. Chem. Soc., Chem. Commun.* **1994**, 2749–2750.

(29) Qiu, S.; Ohnishi, R.; Ichikawa, M. *J. Chem. Soc., Chem. Commun.* **1992**, 1425–1427.

(30) Deka, A.; Deka, R. C.; Choudhury, A. *Chem. Phys. Lett.* **2010**, *490*, 184–188.

(31) Griffe, B.; Brito, J. L.; Sierraalta, A. *J. Mol. Catal. A: Chem.* **2010**, *315*, 28–34.

(32) Sierraalta, A.; Alejos, P.; Ehrmann, E.; Rodriguez, L. J.; Ferrer, Y. *J. Mol. Catal. A: Chem.* **2009**, *301*, 61–66.

(33) Sierraalta, A.; Hernandez-Andara, R.; Ehrmann, E. *J. Phys. Chem. B* **2006**, *110*, 17912–17917.

(34) Sierraalta, A.; Alejos, P.; Ehrmann, E. *Int. J. Quantum Chem.* **2008**, *108*, 1696–1704.

(35) Sierraalta, A.; Añez, R.; Diaz, L.; Gomperts, R. *J. Phys. Chem. A* **2010**, *114*, 6870–6878.

(36) Zhao, Y.; Truhlar, D. G. *J. Chem. Phys.* **2006**, *125*, 194101–194118.

(37) Zhao, Y.; Truhlar, D. G. *Acc. Chem. Res.* **2008**, *41*, 157–167.

(38) Zhao, Y.; Truhlar, D. G. *Theor. Chem. Acc.* **2008**, *120*, 215–241.

(39) Olson, D. H.; Dempsey, E. *J. Catal.* **1969**, *13*, 221–231.

(40) Drake, I. J.; Zhang, Y.; Gilles, M. K.; Teris Liu, C. N.; Nachimuthu, P.; Perera, R. C. C.; Wakita, H.; Bell, A. T. *J. Phys. Chem. B* **2006**, *110*, 11665–11676.

(41) Dolg, M.; Wedig, U.; Stoll, H.; Preuss, H. *J. Chem. Phys.* **1986**, *86*, 866–872.

(42) Valero, R.; Gomes, J. R. B.; Truhlar, D. G.; Illas, F. *J. Chem. Phys.* **2008**, *129*, 124710.

(43) Valero, R.; Gomes, J. R. B.; Truhlar, D. G.; Illas, F. *J. Chem. Phys.* **2010**, *132*, 124710.

(44) Valero, R.; Costa, R.; De P. R. Moreira, I.; Truhlar, D. G.; Illas, F. *J. Chem. Phys.* **2008**, *128*, 114103.

(45) Zhao, Y.; Truhlar, D. G. *J. Phys. Chem. C* **2008**, *112*, 6860–6868.

(46) Zhao, Y.; Truhlar, D. G. *J. Chem. Theory Comput.* **2009**, *5*, 324–333.

(47) Zheng, J.; Zhang, S.; Truhlar, D. G. *J. Phys. Chem. A* **2008**, *112*, 11509–11513.

(48) Boekfa, B.; Choomwattana, S.; Khongpracha, P.; Limtrakul, J. *Langmuir* **2009**, *25*, 12990–12999.

(49) Kumsapaya, C.; Bobuatong, K.; Khongpracha, P.; Tantirungrotechai, Y.; Limtrakul, J. *J. Phys. Chem. C* **2009**, *113*, 16128–16137.

(50) Maihom, T.; Boekfa, B.; Sirijaraensre, J.; Nanok, T.; Probst, M.; Limtrakul, J. *J. Phys. Chem. C* **2009**, *113*, 6654–6662.

(51) Maihom, T.; Pantu, P.; Tachakritikul, C.; Probst, M.; Limtrakul, J. *J. Phys. Chem. C* **2010**, *114*, 7850–7856.

(52) Wannakao, S.; Boekfa, B.; Khongpracha, P.; Probst, M.; Limtrakul, J. *ChemPhysChem* **2010**, *11*, 3432–3438.

(53) Gonzalez, C.; Schlegel, H. B. *J. Chem. Phys.* **1989**, *90*, 2154–2161.

(54) Schlegel, H. B. *J. Comput. Chem.* **1982**, *3*, 214–218.

(55) Reed, A. E.; Curtiss, L. A.; Weinhold, F. *Chem. Rev.* **1988**, *88*, 899–926.

(56) Reed, A. E.; Weinhold, F. *J. Chem. Phys.* **1983**, *78*, 4066–4073.

(57) Frisch, M. J.; Trucks, G. W.; Schlegel, H. B.; Scuseria, G. E.; Robb, M. A.; Cheeseman, J. R.; Montgomery, J. A., Jr; Vreven, T.; Kudin, K. N.; Burant, J. C.; Millam, J. M.; Iyengar, S. S.; Tomasi, J.; Barone, V.; Mennucci, B.; Cossi, M.; Scalmani, G.; Rega, N.; Petersson, G. A.; Nakatsuji, H.; Hada, M.; Ehara, M.; Toyota, K.; Fukuda, R.; Hasegawa, J.; Ishida, M.; Nakajima, T.; Honda, Y.; Kitao, O.; Nakai, H.; Klene, M.; Li, X.; Knox, J. E.; Hratchian, H. P.; Cross, J. B.; Adamo, C.; Jaramillo, J.; Gomperts, R.; Stratmann, R. E.; Yazyev, O.; Austin, A. J.; Cammi, R.; Pomelli, C.; Ochterski, J. W.; Ayala, P. Y.; Morokuma, K.; Voth, G. A.; Salvador, P.; Dannenberg, J. J.; Zakrzewski, V. G.; Dapprich, S.; Daniels, A. D.; Strain, M. C.; Farkas, O.; Malick, D. K.; Rabuck, A. D.; Raghavachari, K.; Foresman, J. B.; Ortiz, J. V.; Cui, Q.; Baboul, A. G.; Clifford, S.; Cioslowski, J.; Stefanov, B. B.; Liu, G.; Liashenko, A.; Piskorz, P.; Komaromi, I.; Martin, R. L.; Fox, D. J.; Keith, T.; Al-Laham, M. A.; Peng, C. Y.; Nanayakkara, A.; Challacombe, M.; Gill, P. M. W.; Johnson, B.; Chen, W.; Wong, M. W.; Gonzalez, C.; Pople, J. A. *Gaussian 03*, revision B.05; Gaussian, Inc.: Pittsburgh, PA, 2003.

(58) Datka, J.; Kozyra, P.; Kukulska-Zajac, E.; Kobyzewa, W. *Catal. Today* **2005**, *101*, 117–122.

(59) Broclawik, E.; Zalucka, J.; Kozyra, P.; Mitoraj, M.; Datka, J. *Catal. Today* **2011**, *169*, 45–51.

(60) Yang, Q.; Tong, X.; Zhang, W. *J. Mol. Struct. (THEOCHEM)* **2010**, *957*, 84–89.

(61) Injan, N.; Pannorad, N.; Probst, M.; Limtrakul, J. *Int. J. Quantum Chem.* **2005**, *105*, 898–905.

(62) Boekfa, B.; Pantu, P.; Limtrakul, J. *J. Mol. Struct.* **2008**, *889*, 81–88.

(63) Jansang, B.; Nanok, T.; Limtrakul, J. *J. Mol. Catal. A: Chem.* **2007**, *264*, 33–39.

(64) Maihom, T.; Namuangruk, S.; Nanok, T.; Limtrakul, J. *J. Phys. Chem. C* **2008**, *112*, 12914–12920.

(65) Sirijaraensre, J.; Limtrakul, J. *Phys. Chem. Chem. Phys.* **2009**, *11*, 578–585.